International Journal of Innovation and Industrial Revolution
EISSN: 2637-0972
IJIREV
Volume: 8 Issue: 24 (March 2026) PP. 357-371

INTERNATIONAL JOURNAL OF INNOVATION AND INDUSTRIAL REVOLUTION (IJIREV)
www.gaexcellence.com/ijirev

GLOBAL ACADEMIC EXCELLENCE

DIRECTIONAL EFFECTS IN ROBOTIC MILLING OF UHMWPE: AN EMPIRICAL STUDY ON SURFACE ROUGHNESS

Wan Nor Shela Ezwane Wan Jusoh[1], Mohamad Irwan Yahaya[2]*, Shukri Zakaria[3], Mahamad Hisyam Mahamad Basri[4], Md Razak Daud[5]

[1] Faculty of Mechanical Engineering, UiTM Penang Branch, Permatang Pauh Campus, 13500 Permatang Pauh, Penang, Malaysia
2024829196@student.edu.my https://orcid.org/0009-0004-8779-6896
[2] Faculty of Mechanical Engineering, UiTM Penang Branch, Permatang Pauh Campus, 13500 Permatang Pauh, Penang, Malaysia
irwan352@uitm.edu.my https://orcid.org/0000-0002-4595-1411
[3] Faculty of Mechanical Engineering, UiTM Penang Branch, Permatang Pauh Campus, 13500 Permatang Pauh, Penang, Malaysia
2024321221@student.edu.my https://orcid.org/0009-0006-8371-806X
[4] Faculty of Mechanical Engineering, UiTM Penang Branch, Permatang Pauh Campus, 13500 Permatang Pauh, Penang, Malaysia
mhisyam.mbasri@uitm.edu.my https://orcid.org/0000-0001-9804-5271
[5]Mechanical Engineering Department, Politeknik Ibrahim Sultan, 81700 Pasir Gudang, Johor Darul Ta'zim, Malaysia
razakat@gmail.com https://orcid.org/0000-0002-9032-8274
*Corresponding Author

Article Info:

Article history:
Received date: 29.12.2025
Revised date: 15.01.2026
Accepted date: 11.02.2026
Published date: 18.03.2026

Abstract:

Industrial robots offer large workspaces and flexibility for machining, but their compliance-dominated dynamics can compromise surface quality. While vibration control in robotic machining is well studied for metals and fibre-reinforced composites, empirical guidance for soft-polymer finishing remains limited. As one of the first empirical studies on robotic finishing of UHMWPE, this work investigates the direction–

International Journal of Innovation and Industrial Revolution
IJIREV
EISSN: 2637-0972
Volume: 8 Issue: 24 (March 2026) PP. 357-371

To cite this document:

Wan Jusoh, W. N. S. E., Yahaya, M. I., Zakaria, S., Mahamad Basri, M. H., & Daud, M. R. (2026). Directional Effects in Robotic Milling of UHMWPE: An Empirical Study on Surface Roughness. *International Journal of Innovation and Industrial Revolution, 8* (24), 357-371.

compliance–roughness interaction by framing feed direction as a controllable parameter. This study explicitly demonstrates how feed direction interacts with pose-dependent compliance to systematically influence surface roughness in robotic milling of UHMWPE. This feasibility study investigates how feed direction affects surface roughness (Ra, Rq, Rz) in robotic milling of UHMWPE. Experiments were performed using a KUKA KR120 R2700 six-axis robot with fixed parameters: 9500 rpm spindle speed, 1080 mm/min feed rate, and dry finishing cuts at depths of 0.1, 0.2, and 0.3mm. Surface roughness metrics were measured via contact profilometry using a standardized evaluation length. Due to kinematic constraints, X–Y toolpaths require different joint configurations; therefore, observed differences reflect the combination of feed-direction and pose-dependent stiffness anisotropy. Y-direction feeding produced lower Ra (1.64–1.87 μm) than X-direction feeding (1.66–1.94 μm). In contrast, X-direction feeding yielded lower Rq (2.0–2.5 μm) with strong linear predictability ($R^2 >$ 0.99), compared with Y-direction Rq (2.35–2.40 μm). Rz exhibited depth-dependent behavior, with X performing better at shallow depth (0.2 mm) and Y at 0.3 mm, while tool adhesion showed little directional dependence. Overall, the findings provide evidence of direction-dependent roughness trade-offs: Y-direction may be preferred for average smoothness (Ra), whereas X-direction may be preferred when peak-sensitive control (Rq/Rz) is critical.

DOI: 10.35631/IJIREV.824022

Keyword:

Feed Direction, Pose-Dependent Compliance, Robotic Milling, Surface Roughness (Ra, Rq, Rz), UHMWPE

Introduction

The use of industrial robots in machining has grown due to their large workspace, multi-axis capability, and comparatively lower investment cost relative to dedicated multi-axis CNC machine tools (Wang et al., 2023). Recent reviews highlight that robotic machining enables processing of large and complex parts which facilitates flexible cell reconfiguration for low- to medium-volume production. However, these advantages are accompanied by limited structural rigidity and posture-dependent dynamics. Despite its growing importance in medical and industrial applications, this study presents one of the first empirical investigations into the robotic finishing of Ultra-High Molecular Weight Polyethylene (UHMWPE), a soft polymer known for its challenging machinability. The novelty of this work lies in the explicit characterisation of the interaction between feed direction and robot compliance, and how this relationship dictates surface roughness. A core contribution that addresses a significant gap in current robotic manufacturing literature.

International Journal of Innovation and Industrial Revolution
IJIREV
EISSN: 2637-0972
Volume: 8 Issue: 24 (March 2026) PP. 357-371

In serial robots, structural stiffness is not uniform across the workspace, leading to posture-dependent dynamics (Wen et al., 2023). This pose-dependent stiffness anisotropy directly affects the tool–workpiece interaction, giving rise to compliance-dominated dynamics that can degrade surface quality, particularly during finishing operations. While existing studies primarily emphasise the optimisation of conventional process parameters such as spindle speed and feed rate, the role of feed direction relative to the robot's stiffness distribution remains a critical yet underexplored controllable factor in robotic machining. This limitation is further amplified when machining soft polymers such as UHMWPE, where the material's low elastic modulus increases sensitivity to directional compliance effects. Therefore, this study positions feed direction as a strategic geometric parameter to mitigate the influence of robot compliance on surface roughness and machining precision.

Vibration and chatter are therefore widely recognised as major challenges in robotic machining, affecting dimensional accuracy, surface integrity, and tool life. Guo et al. (2022), Liu et al. (2022), and Sun et al. (2023) illustrate different suppression strategies: active contact milling to stabilise machining without overly conservative parameters (Guo et al., 2022), redundant degree-of-freedom optimisation to obtain chatter-free cutting depth (Y. Liu et al., 2022), and transfer-learning approaches to predict stability boundaries across tool–workpiece combinations (Sun et al., 2023). Together, these works indicate a move toward adaptive and configuration-aware approaches, but practical deployment still requires empirical understanding of how robot dynamics interact with specific material classes and surface-quality targets.

Accordingly, recent studies emphasise the importance of modelling and analysing robot structural dynamics and vibration behaviour in milling (Joshi et al., 2024). Chatter and vibration are well known to influence surface roughness and machining sustainability (Abellán-Nebot et al., 2024). Prior research in robotic milling shows that machining configuration (robot position, spindle orientation, tool overhang) and process parameters (spindle speed, feed rate, depth of cut) jointly influence vibration severity and stability (Cordes et al., 2019; Ji et al., 2024; Mohammadi et al., 2022). Most robotic milling studies have focused on metals and the trimming of fibre-reinforced composites. In contrast, fewer empirical studies examine soft engineering polymers under robotic milling, where even modest cutting forces can still excite compliance-driven vibration that affects surface integrity. Table 1 summarises representative studies on robotic milling of metals and composites to contextualise this work and highlight the limited evidence base for soft engineering polymer milling.

Table 1: Representative Studies on Robotic Milling of Metals and Composites: Evidence of Limited Work on Soft Engineering Polymers

Author/ Year	Machine	Machining Strategy	Material	Surface Roughness (µm)
(J. Liu et al., 2024)	Six-axis industrial robot with high-speed spindle (custom robotic milling setup)	Ball-end milling, posture-dependent vibration analysis, dry milling	Aluminum alloy 7075-T6	0.1 – 0.8 depending on posture and parameters
(Yan et al., 2024)	KUKA KR500 robot + ES779	Additive–subtractive hybrid manufacturing, HASM	WAAM-fabricated	2.013 (best surface quality)

International Journal of Innovation and Industrial Revolution
EISSN: 2637-0972 IJIREV
Volume: 8 Issue: 24 (March 2026) PP. 357-371

	high-speed milling head		Al-alloy (5052 series)	
(Ni et al., 2022)	Robot Mitsubishi RV-4FRL-1D-S11 with spindle NAKANISHI (max 30,000 rpm)	Flat-end milling (contouring finishing) Fixed robot posture	7075-T651 aluminium alloy (high-strength aerospace grade)	0.374 – 3.131
(Da Silva et al., 2019)	8-axis robotic milling system (Motoman SV3X + 2-axis worktable, EM25N-5000-J4 spindle)	Rough cut (zigzag tool path, posture chosen to avoid collisions) Finish cut (zigzag contour, tool orientation optimized using stiffness indices)	ABS chemical wood	~0.5 mm error (surface irregularities, not reported in µm)
(Mousavi et al., 2018)	ABB IRB6660 industrial robot + Fischer MFW 1412/36 spindle (max 36,000 rpm)	Slot milling along straight trajectory, posture optimized via functional redundancy	Aluminum	2.5 - 11

The current review affirms that soft engineering polymers are still unexplored in spite of the development of robotic milling of rigid materials. Notwithstanding the focus of robotic machining studies on metals and composites, UHMWPE has concurrently become a vital engineering polymer in biomedical, tribological, and many applications due to its superior wear resistance, low friction, and remarkable impact strength. Despite its attractive properties, UHMWPE remains notorious for the challenges of producing high-quality surfaces during machining. The combination of low thermal conductivity and comparatively low melting temperature encourages local heating and smearing, whereas the ductile nature of it encourages the development of continuous chips, burrs on the edges and accumulated material sticking to the cutting tool. Most studies on machining UHMWPE materials have used CNC machines as summarised in Table 2. From the observations of previous studies, spindle speed, feed rate and depth of cut have significant effects on surface roughness, burr formation and cutting force. In addition, surface finish can also be achieved depending on sharp tools, limited depth of cut and precise adjustment of chip load.

Table 2: Summary Of CNC Milling Studies on UHMWPE Surface Roughness Optimization

Author/ Year	Machine	Material	Spindle Speed (rpm)	Feed Rate (mm/min)	Depth of Cut (mm)	Surface Roughness µm
(Piska & Urbancova, 2022)	CNC milling	UHMWPE	764	315, 450, 630	1	0.774
(Lopes et al., 2021)	CNC milling	UHMWPE	9500	1767	0.035 – 0.110	0.82 – 3.38 Optimum: 1.13

(Lestari et al., 2019)	CNC milling	UHMWPE	6500 – 7500	1000 – 2000	-	0.57 – 1.75 optimum: 0.143

Prior CNC-based findings generally indicate that spindle speed, feed rate, and depth of cut influence surface roughness, burr formation, and cutting force, and that surface finish can be improved using sharp tools, shallow cuts, and controlled chip load. However, empirical characterisation and optimisation of UHMWPE cutting parameters under robotic milling aim on the measurement and quality of surface finish.

This paper addresses the identified gap through an experimental investigation of robotic UHMWPE milling, focusing on the effect of feed direction on surface roughness under low vibration finishing conditions. This study is guided by two research objectives: to analyze the influence of feed direction (Y-axis versus X-axis) on surface roughness parameters (Ra, Rq, Rz), and to determine whether directional effects are dependent on depth of cut (0.1–0.3 mm). Ni et al. (2022) reported that feeding along the Y direction produced lower vibration and improved surface outcomes compared with the X direction, attributed to direction-dependent stiffness in serial robots (Ni et al., 2022). Building on this motivation, the present work provides a feasibility assessment of whether similar directional tendencies are observed for UHMWPE surface finishing under posture-controlled conditions.

To reduce vibration-related confounding from aggressive cutting, the experiments employ shallow finishing passes, short tool overhang, and a constant robot posture within each feed direction (Lai et al., 2024). Notably, due to kinematic constraints, X- and Y-direction toolpaths require different joint configurations; therefore, any observed X–Y differences should be interpreted as combined effects of feed direction and pose-dependent compliance. The results are presented as preliminary evidence intended to inform subsequent optimisation studies with larger sample sizes and inferential statistical analysis.

Methodology

Materials and Workpiece Preparation

Ultra-high molecular weight polyethylene (UHMWPE) was selected as the workpiece material to evaluate robotic milling as a potential alternative to CNC finishing for soft polymers. The UHMWPE stock provided by Röchling Engineering Plastics Sdn. Bhd. is a neat thermoplastic with low thermal conductivity and viscoelastic behaviour that can promote heat build-up and elastic recovery during milling. Test specimens (50 × 50 × 50 mm) were cut from as-received stock, deburred, and conditioned for 24 h at 23 ± 2 °C and 50 ± 5% relative humidity in accordance with ISO 291:2008. Table 3 summarises the key thermomechanical properties used to define conservative process limits and reduce the risk of thermal softening and smearing during finishing trials. Accordingly, the finishing parameter window in this study employed shallow axial depths of cut (0.1–0.3 mm) to limit heat accumulation and smearing in UHMWPE. This conservative range is consistent with prior UHMWPE machining studies that recommend shallow finishing cuts and controlled chip load to improve surface quality (Lopes et al., 2021) (Lestari et al., 2019). All trials were performed under dry cutting to reflect practical robotic cells without coolant delivery and to avoid confounding from coolant-driven thermo-mechanical changes in UHMWPE.

International Journal of Innovation and Industrial Revolution
EISSN: 2637-0972
IJIREV
Volume: 8 Issue: 24 (March 2026) PP. 357-371

Table 3: UHMWPE Material Properties Used in The Experiment

Properties	Value	Unit
Density	0.93	g/cm^3
Yield Stress	20	MPa
Tensile Modulus of Elasticity	680	MPa
Melting Temperature	135	°C
Heat Deflection Temperature	79	°C
Coefficient of Thermal Expansion	150-230	$\times 10^{-6}$ K^{-1}
Dielectric Strength	45	kV/mm

Simulation Setup

SprutCAM simulation serves as a vital step in robotic machining virtual workflows to validate toolpaths, assess robot kinematics, and detect potential collisions prior to physical trials. The path programming joint axes are also defined as the kinematic chain (A1-A6) and tool-fixed coordinate frame. Figure 1 shows the interface and simulation of Sprutcam software.

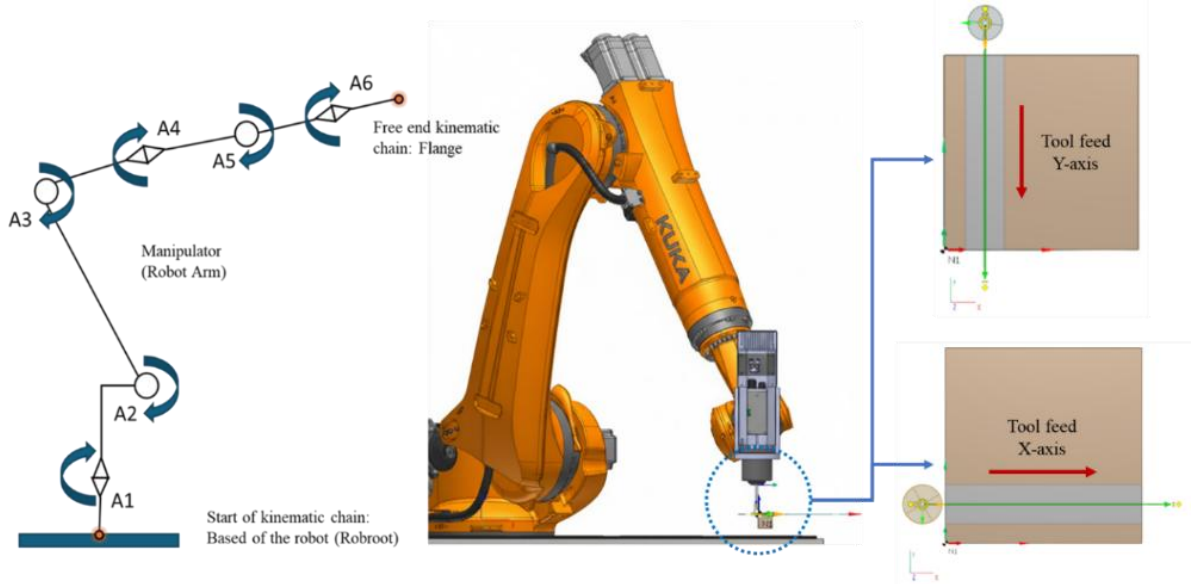

Figure 1: Simulation Sprutcam to Simulate Different Tool Feed Direction

The joint angles shown in Table 4 were fixed at all depths in each direction of feed (X-feed and Y-feed), as no posture comparisons is made across depths in a direction. The X-feed and Y-feed positions are different due to the fact that various joint setups are required to achieve the two toolpath directions. This pre-experimental validation is particularly important in robotic manufacturing due to the multi-dimensional nature of six-axis motion. Furthermore, the nature of the interaction between the toolpath and the material geometry creates the need to perform an extensive validation process. This approach aims to obtain accurate machining results without compromising operational efficiency and safety standards (Wan Jusoh et al., 2025).

International Journal of Innovation and Industrial Revolution
EISSN: 2637-0972 IJIREV
Volume: 8 Issue: 24 (March 2026) PP. 357-371

Table 4: Robot Kinematic Chain

Axis	Joint	Angular Value (°)	
		X-axis feed direction	Y-axis feed direction
A1	Joint 1	46.573	47.764
A2	Joint 2	−69.762	−70.614
A3	Joint 3	129.999	129.482
A4	Joint 4	-47.476	133.314
A5	Joint 5	-68.868	67.494
A6	Joint 6	21.46	−157.903

Experimental Setup

A KUKA KR120 R2700 industrial robot (QUANTEC series, KUKA Robotics, Augsburg, Germany) equipped with a high-speed spindle (GDL70-24Z/9.0, HQD Mechatronic Division, Changzhou, China) was employed for the milling experiments. The robot features a high workstation capacity and nominal repeatability of ±0.05 mm in accordance with ISO 9283, with detailed specifications relevant to path precision and load capacity provided in Table 5. To isolate the effects of feed direction and depth of cut, spindle speed and feed rate were held constant at 9500 rpm and 1080 mm/min. Each condition was machined once (single pass per setting) in this feasibility study. Replication was therefore performed at the measurement level (n = 3 profilometer locations per condition), rather than through repeated machining runs.

Table 5 Specification of Kuka KR120 R2700 (Wan Jusoh et al., 2025)

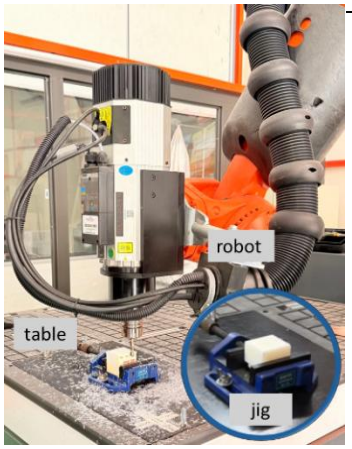

Parameter	Value	Unit
Maximum reach	2701	mm
Rated payload	120	kg
Maximum payload	167	kg
Maximum supplementary load, rotating column / link arm / arm	300 / 130 / 150	kg
Pose repeatability (ISO 9283)	± 0.05	mm
Number of axes	6	-
Mounting position	Floor	-
Footprint	754 x 754	mm
Weight approx.	1069	kg

A high-speed spindle equipped with a 10 mm two-flute HSS flat end mill was used in all experiments. The machining parameters were fixed at 9500 rpm spindle speed and 1080 mm/min feed rate, while depth of cut and feed direction were varied to assess their effects on surface roughness. The block of UHMWPE was placed in a mechanical vice that was attached to the table of the robot cell, and the clamping layout remained the same throughout the experiments. A Tool Center Point (TCP) was assigned to the end of the mill geometry. A tool pressenter procedure on a flat reference surface was used to measure the tool length and setting

International Journal of Innovation and Industrial Revolution
IJIREV
EISSN: 2637-0972
Volume: 8 Issue: 24 (March 2026) PP. 357-371
coordinates. The same TCP (X 300.33 Y 0.09 Z 85.41 with a tool overhang of 74.46mm) was set in Sprutcam to ensure the accuracy of tool tip in Z position before machining.

The coordinate system of the workpiece was referred to the UHMWPE block. The origin was put at the upper left front corner of the block, the X and Y axes were parallel with the long and short sides of the workpiece respectively and the Z axis was at right angles to the robot surface. Position of the workpiece was X 974.86 Y -1406.31 Z 411.69. The workpiece base was set identically in SprutCAM and the robot controller to ensure that the programmed toolpath corresponded precisely with the actual machining operation. To compare the feed direction, the sole programmed variation was the toolpath direction, set either along +Y or −X. There were no changes in the TCP and workpiece base positions. Prior to the finishing tests, the upper surfaces for all UHMWPE blocks were face-milled using the same spindle-tool combination to obtain a flat reference surface. Multiple over-lapping passes were executed to remove the saw-cut layer and establish a flat reference surface. Face milling was then applied, and the Z0 of the workpiece coordinate system was defined on this planar surface.

The finishing experiments were then conducted on this prepared face at shallow depths of cut (0.1, 0.2 and 0.3 mm). For each run, a straight contour pass was executed at the chosen depth in both feed directions (Y-axis and –X-axis) to enable comparison of directional effects. The robot joint (A1-A6) was kept constant at all cutting depth levels (i.e., posture was held constant within each feed direction but differs between the X- and Y-direction toolpaths) but the joint arrangement is not the same in the X- and Y-feed toolpaths because of kinematic limitations. Therefore, any observed X–Y differences should be interpreted as combined effects of feed direction and pose-dependent compliance. Joint angles were held constant across depths within each feed direction; however, due to kinematic constraints, X- and Y-direction toolpaths required different joint configurations. The measurement of surface roughness was made at the three points of each machine track, slightly outside the lead-in and lead-out segment tracks, to eliminate lead-in/lead-out effects and the error bars plotted are ±1 standard deviation (SD). For each condition, n = 3 profilometer measurements were taken along the machined pass, and the reported ±1 SD represents within-pass measurement variability rather than replicate machining runs. The measurements were obtained using a Mitutoyo SJ-401 contact stylus profilometer (Mitutoyo Corporation, Kawasaki, Japan) with cut-off length λ_c, 0.8, and evaluation length, 4.0 mm ($5\lambda_c$).

Result And Discussion

All findings reported in this section should be interpreted as preliminary trends under the tested robot configurations and fixturing conditions, rather than universal directional effects. The observed superiority of Y-axis feed in achieving lower average surface roughness is consistent with the findings of Ni et al. (2022), who reported that Y-direction feeding can reduce vibration levels compared to X-direction due to directional stiffness variation in serial robotic systems. Taking together, these observations suggest that surface quality in robotic milling is shaped not only by cutting parameters but also by direction- and pose-dependent robot compliance (Ni et al., 2022). In the present study, X–Y toolpaths required different joint configurations; therefore, the observed difference should be interpreted as a practical combined effect of feed direction and pose-dependent stiffness rather than a purely directional effect.

International Journal of Innovation and Industrial Revolution
IJIREV
EISSN: 2637-0972
Volume: 8 Issue: 24 (March 2026) PP. 357-371

Figure 2 shows the effect of feed direction on surface roughness across all cutting depths. The Y-axis feed produced lower Ra values (1.642–1.867 µm) compared to the X-axis feed (1.661–1.936 µm). Within this feasibility dataset, the consistent offset across depths indicates a repeatable difference between the two toolpath configurations, unlikely to be solely due to within-pass measurement variability. Both feed directions exhibited a strong linear correlation with depth of cut ($R^2 > 0.93$) across the three tested depths, and Ra increased approximately linearly with increasing cutting depth. This trend suggests no obvious nonlinearity in the Ra response within the investigated depth range, although confirming cutting-regime stability would require additional evidence such as force or vibration measurements, or chip morphology, as commonly emphasized in machining stability studies (Li et al., 2023). X-axis feed demonstrated higher predictability ($R^2 = 0.9981$) compared to Y-axis feed ($R^2 = 0.9333$). This indicates that, under the tested configuration, the X-axis condition produced a more consistent linear Ra–depth relationship, albeit with higher sensitivity to depth changes. This behaviour may be consistent with direction- and pose-dependent compliance effects in serial robots (Ni et al., 2022), but confirming the underlying mechanism would require direct stiffness or vibration characterization, as emphasized by Wu et al. (2022) in their review of industrial robot stiffness identification and modelling (Wu et al., 2022). Finally, the separation between directions appears more pronounced at the deeper cut (0.3 mm), while overlapping error bars at shallow depths (0.1–0.2 mm) suggest the practical benefit may be modest under low-load finishing, within the reported measurement variability.

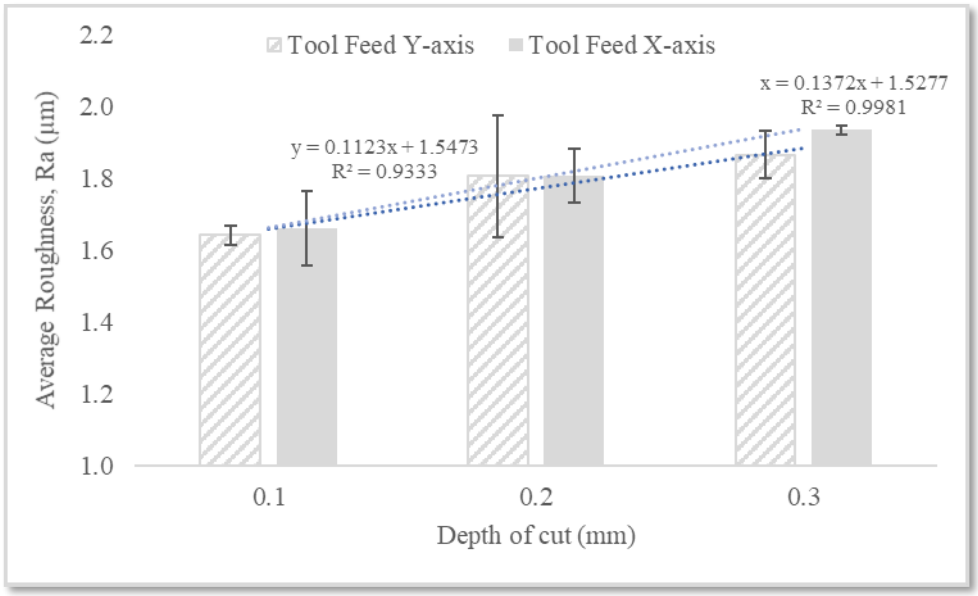

Figure 2 Effect of Depth of Cut on Average Surface Roughness (Ra) For Y-Axis And X-Axis Feed Directions (Single Machining Pass Per Condition; N = 3 Profilometer Measurements Per Track; Error Bars = ±1 SD)

In contrast to the Ra trends, Figure 3 shows that X-axis feed achieved lower Rq values (2.0–2.5 µm) than Y-axis feed (2.35–2.40 µm) across the tested depths. Rather than being contradictory, this separation between Ra and Rq responses suggests that directional effects may influence peak-sensitive roughness differently from average roughness. The Y-axis condition showed a weak depth–Rq relationship ($R^2 = 0.5396$), with comparatively larger variability at the shallow cut (0.1 mm), whereas the X-axis condition exhibited an almost perfectly linear increase of Rq with depth ($R^2 = 0.9996$) across the three tested depths. Within this pilot dataset, these trends indicate that X-axis feeding produced a stronger, more consistent

International Journal of Innovation and Industrial Revolution
IJIREV
EISSN: 2637-0972
Volume: 8 Issue: 24 (March 2026) PP. 357-371

linear Rq–depth response, while Y-axis feeding displayed greater scatter in peak-sensitive roughness.

Taken together, the results are consistent with the interpretation that Y-axis feed can yield lower average surface heights (Ra) yet show higher sensitivity to occasional surface irregularities captured by Rq, whereas X-axis feed may reduce peak-sensitive roughness and improve predictability under the tested configuration. This distinction is expected because Rq is more sensitive to larger height deviations than Ra and therefore can reflect peak-dominated behaviour that may not shift the mean roughness appreciably. Because X–Y toolpaths required different joint configurations in this study, the observed contrast should be interpreted as a practical combined effect of feed direction and pose-dependent compliance, rather than a purely directional effect. Further work with posture-matched paths and direct vibration and stiffness measurements would help confirm the underlying mechanism.

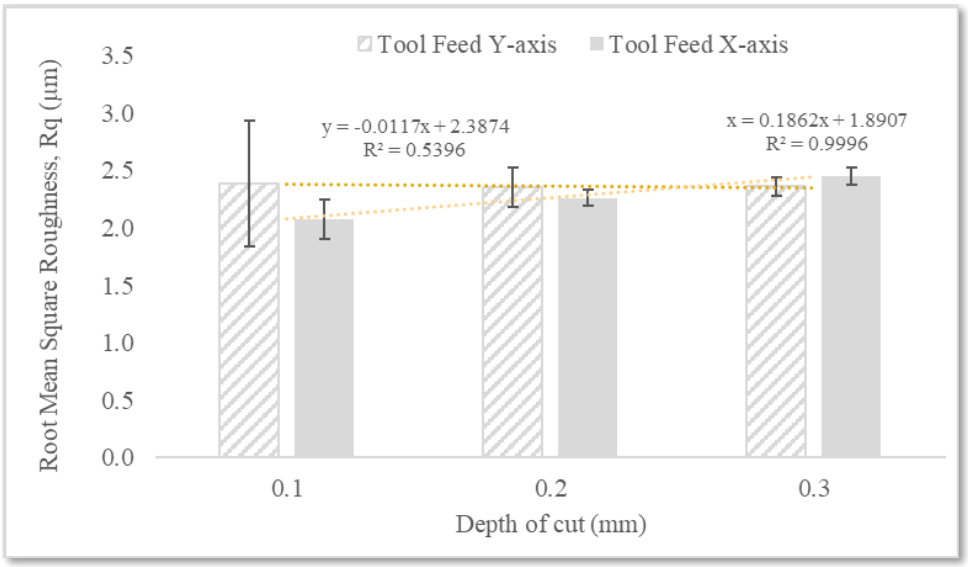

Figure 3: Effect Of Depth of Cut on Root Mean Square Roughness (Rq) For Y-Axis and X-Axis Feed Directions (Single Machining Pass Per Condition; N = 3 Profilometer Measurements Per Track; Error Bars = ±1 SD)

Figure 4 shows a depth-dependent directional behaviour for Rz. At the shallow depth of cut (0.1 mm), both feed directions produced comparable Rz values (9.18 µm for X-axis and 8.99 µm for Y-axis), suggesting that peak-to-valley height is only weakly separated by direction under low-load finishing. At the intermediate depth (0.2 mm), X-axis feed yielded a lower Rz value (10.23 µm) than Y-axis feed (11.99 µm). However, at the deepest cut (0.3 mm), the directional advantage shifted, with Y-axis feed producing a lower Rz value (11.01 µm) than X-axis feed (11.82 µm). Within this feasibility dataset, this crossover indicates that the relative Rz performance between directions can change with depth of cut. This suggests that, when Rz is used as the acceptance criterion for finishing quality, feed-direction selection should be made in conjunction with the intended finishing depth, instead of assuming a fixed directional preference.

Linear fitting further highlights a difference in predictability: the X-axis condition shows a strong correlation with depth of cut ($R^2 = 0.9949$), whereas the Y-axis condition exhibits weak correlation ($R^2 = 0.4108$). This contrast suggests that the X-axis configuration produced a more

International Journal of Innovation and Industrial Revolution
EISSN: 2637-0972
IJIREV
Volume: 8 Issue: 24 (March 2026) PP. 357-371

consistent peak-to-valley response across the tested depths, while the Y-axis configuration displayed greater variability in peak-sensitive behaviour. Because X–Y toolpaths required different joint configurations in this study, these findings should be interpreted as combined effects of feed direction and pose-dependent compliance rather than a purely directional effect. Practically, the higher predictability observed for the X-axis condition may support more reliable process planning when consistency is prioritised, while the depth-dependent crossover indicates that directional selection for Rz may depend on the finishing depth used.

While the absolute differences in Ra between the X and Y feed directions were modest, the results reveal a clear and systematic trade-off between the roughness metrics. Rq and Rz exhibited strong direction-dependent predictability, particularly in the X-direction where linear correlation remained exceptionally high ($R^2 > 0.99$). This suggests that the differences observed are not random variations but are systematic effects of the pose-dependent stiffness anisotropy. Consequently, this study identifies an application-specific trade-off: Y-axis feeding is preferred when average smoothness (Ra) is the priority, whereas X-axis feeding offers superior predictability and control over peak-sensitive metrics (Rq and Rz).

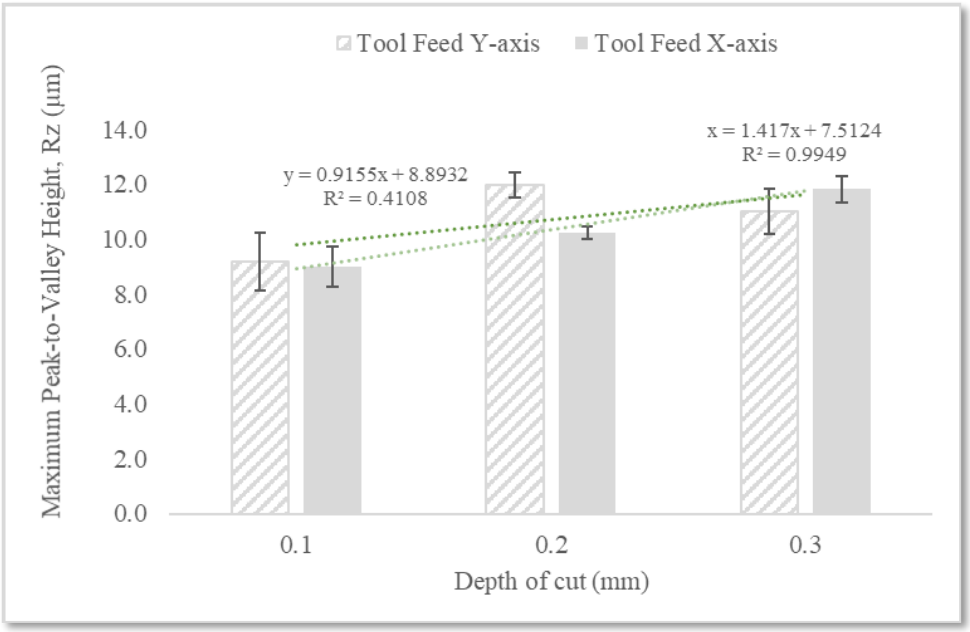

Figure 4: Effect Of Depth of Cut on Maximum Peak-To-Valley Height (Rz) For Y-Axis and X-Axis Feed Directions (Single Machining Pass Per Condition; N = 3 Profilometer Measurements Per Track; Error Bars = ±1 SD)

As no inferential statistics were performed and X–Y toolpaths required different joint configurations in this study, these findings must be interpreted as a combined effect of feed direction and pose-dependent stiffness anisotropy. Accordingly, the observed roughness trends should not be attributed to feed direction alone but rather understood as robot-specific responses arising from kinematic constraints and posture-dependent compliance. These preliminary trends within this pilot dataset motivate future work, which should involve validation through posture-matched paths and larger experimental replication to further isolate the effects of stiffness anisotropy on the machining of soft polymers.

International Journal of Innovation and Industrial Revolution
IJIREV
EISSN: 2637-0972
Volume: 8 Issue: 24 (March 2026) PP. 357-371

Figure 5 documents the tool condition after finishing passes at depths of cut of 0.1, 0.2, and 0.3 mm. At 0.1 mm, the flank face and tool corner appear largely free of visible wear, with only minimal UHMWPE adhesion. As the depth of cut increases to 0.2–0.3 mm, adhered material becomes more evident around the tool corner, indicating greater material build-up under higher engagement conditions. This trend is consistent with increased tool–workpiece contact and frictional interaction as depth increases, which can promote adhesive transfer in soft polymers such as UHMWPE.

No pronounced directional dependency was apparent in the adhesion patterns within the available images; tools used for Y-axis and X-axis feeds showed broadly comparable build-up at the same depth levels. This suggests that, under the investigated finishing conditions, visible adhesion is primarily depth-associated rather than direction-associated. When considered alongside the roughness results, these observations support the interpretation that directional differences in Ra/Rq/Rz are not driven mainly by gross changes in adhesion at the tool corner within this depth range. Nevertheless, confirming the underlying causes would require additional measurements (e.g., temperature, cutting forces, or vibration) beyond post-process tool imaging.

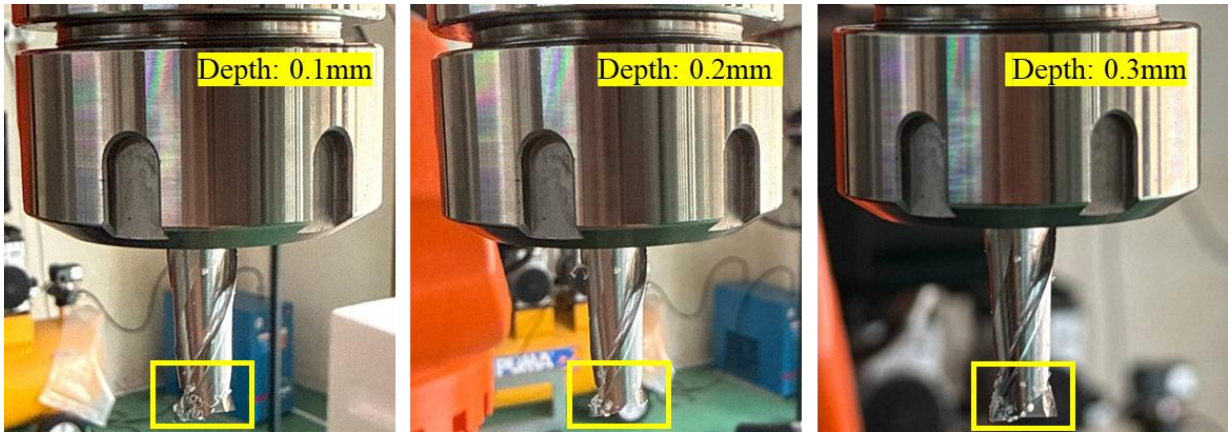

Figure 5: Tool Condition Showing UHMWPE Adhesion at Different Depths Of Cut

Taken together, the Ra, Rq, Rz and tool-adhesion observations indicate that directional differences in robotic milling of UHMWPE are depth-dependent and configuration-sensitive. At shallow depths of cut, both feed directions produced similar peak-to-valley behaviour and only minimal visible adhesion, suggesting limited practical separation between directions under low-load finishing. As depth increases, the roughness metrics diverge: Y-axis feeding tends to favour lower average roughness (Ra), whereas X-axis feeding shows stronger predictability and lower peak-sensitive roughness (Rq), and Rz exhibits a depth-dependent crossover. Meanwhile, visible tool adhesion increases with depth and does not show a pronounced directional contrast within the available images, implying that adhesion in this study is more strongly associated with engagement conditions than with feed orientation. Overall, these results support a condition-specific approach to feed-direction selection in robotic UHMWPE finishing, where depth of cut is a key driver of both roughness magnitude and the extent of directional separation, and where any directional interpretation should be made in the context of pose-dependent compliance.

International Journal of Innovation and Industrial Revolution
EISSN: 2637-0972
Volume: 8 Issue: 24 (March 2026) PP. 357-371

Conclusion

This feasibility study indicates that feed direction can influence UHMWPE surface roughness in robotic milling, with the practical separation between directions varying with depth of cut. Within this pilot dataset and the investigated range, depth of cut appeared to be the primary driver of roughness trends, while directional effects manifested differently across roughness metrics. X-axis feeding was associated with lower peak-sensitive roughness (Rq) and a more predictable response with depth, whereas Y-axis feeding provided a modest advantage in average roughness (Ra). These results are consistent with the view that configuration-dependent compliance in serial robots can affect surface outcomes, highlighting important differences between robotic milling and rigid CNC platforms. Overall, the findings should be interpreted as robot-specific outcomes influenced by the kinematic configuration and pose-dependent compliance examined in this study. Application-specific feed-direction selection is therefore recommended, particularly when balancing average smoothness against peak control and predictability. Future work should evaluate posture-matched toolpaths, pose variability, and broader parameter ranges, supported by direct force and vibration measurements, to establish more comprehensive toolpath optimisation guidelines for polymer machining.

Acknowledgements:	The authors would like to acknowledge the support of Universiti Teknologi Mara (UiTM), Cawangan Pulau Pinang, Malaysia, and Politeknik Tuanku Sultanah Bahiyah, Malaysia, for providing facility support for this research. AI-assisted tools were used to enhance language clarity. All content was authored and verified by the authors.
Funding Statement:	No Funding
Conflict of Interest Statement:	The authors declare that there is no conflict of interest regarding the publication of this paper. All authors have contributed to this work and approved the final version of the manuscript for submission to the International Journal of Innovation and Industrial Revolution (IJIREV).
Ethics Statement:	This study did not involve any human participants, animals, or sensitive data requiring ethical approval. The authors confirm that the research was conducted in accordance with accepted academic integrity and ethical publishing standards.
Author Contribution Statement:	All authors contributed significantly to the development of this manuscript. Wan Nor Shela Ezwane binti Wan Jusoh was responsible for conceptualization, methodology, validation, investigation, formal analysis and writing. Shukri bin Zakaria and Md Razak Daud handled data collection, analysis, and interpretation of results. Mohamad Irwan Yahaya and Mahamad Hisyam Mahamad Basri contributed to the critical revision of the manuscript and overall supervision of the study. All authors read and approved the final version of the manuscript prior to submission.

International Journal of Innovation and Industrial Revolution
IJIREV
EISSN: 2637-0972
Volume: 8 Issue: 24 (March 2026) PP. 357-371

References

Abellán-Nebot, J. V., Vila Pastor, C., & Siller, H. R. (2024). A Review of the Factors Influencing Surface Roughness in Machining and Their Impact on Sustainability. In *Sustainability (Switzerland)* (Vol. 16, Issue 5). Multidisciplinary Digital Publishing Institute (MDPI). https://doi.org/10.3390/su16051917

Cordes, M., Hintze, W., & Altintas, Y. (2019). Chatter stability in robotic milling. *Robotics and Computer-Integrated Manufacturing*, *55*, 11–18. https://doi.org/10.1016/j.rcim.2018.07.004

Da Silva, L. B., Yoshioka, H., Shinno, H., & Zhu, J. (2019). Tool orientation angle optimization for a multi-axis robotic milling system. *International Journal of Automation Technology*, *13*(5), 574–582. https://doi.org/10.20965/ijat.2019.p0574

Guo, K., Zhang, Y., & Sun, J. (2022). Towards stable milling: Principle and application of active contact robotic milling. *International Journal of Machine Tools and Manufacture*, *182*. https://doi.org/10.1016/j.ijmachtools.2022.103952

Ji, Y., & Liu, R. (2024). Research on the influence of cutter overhang length on robotic milling chatter stability. *Scientific Reports*, *14*(1). https://doi.org/10.1038/s41598-024-76165-8

Joshi, R. C., Rai, J. K., Burget, R., & Dutta, M. K. (2024). Optimized inverse kinematics modeling and joint angle prediction for six-degree-of-freedom anthropomorphic robots with Explainable AI. *ISA Transactions*. https://doi.org/10.1016/j.isatra.2024.12.008

Lai, Y. S., Lin, W. Z., Lin, Y. C., & Hung, J. P. (2024). Development of Surface Roughness Prediction and Monitoring System in Milling Process. *Engineering, Technology and Applied Science Research*, *14*(1), 12797–12805. https://doi.org/10.48084/etasr.6664

Lestari, W. D., Anggoro, P. W., Ismail, R., Jamari, J., & Bayuseno, A. P. (2019). Optimization of CNC Milling Parameters through the Taguchi and RSM Methods for Surface Roughness of UHMWPE Acetabular Cup. *International Journal of Mechanical Engineering and Technology (IJMET)*, *10*(2), 1762–1775.

Li, G., Xie, W., Wang, H., Chai, Y., Zhang, S., & Yang, L. (2023). Optimizing Processing Parameters and Surface Quality of TC18 via Ultrasonic-Assisted Milling (UAM): An Experimental Study. *Micromachines*, *14*(6). https://doi.org/10.3390/mi14061111

Liu, J., Niu, Y., Zhao, Y., Zhang, L., & Zhao, Y. (2024). Prediction of Surface Topography in Robotic Ball-End Milling Considering Tool Vibration. *Actuators*, *13*(2). https://doi.org/10.3390/act13020072

Liu, Y., Wang, L., Yu, Y., Zhang, J., & Shu, B. (2022). *Optimization of redundant degree of freedom in robot milling considering chatter stability*. https://doi.org/10.21203/rs.3.rs-1360661/v1

Lopes, F. J., Completo, A., & Davim, J. P. (2021). Toolpath and machining parameters optimisation of the cavities of a knee prosthesis tibial insert. *Proceedings of the Institution of Mechanical Engineers, Part B: Journal of Engineering Manufacture*, *235*(3), 431–442. https://doi.org/10.1177/0954405420961678

Mohammadi, Y., & Ahmadi, K. (2022). Chatter in milling with robots with structural nonlinearity. *Mechanical Systems and Signal Processing*, *167*. https://doi.org/10.1016/j.ymssp.2021.108523

Mousavi, S., Gagnol, V., Bouzgarrou, B. C., & Ray, P. (2018). Stability optimization in robotic milling through the control of functional redundancies. *Robotics and Computer-Integrated Manufacturing*, *50*, 181–192. https://doi.org/10.1016/j.rcim.2017.09.004

Ni, J., Dai, R., Yue, X., Zheng, J., & Feng, K. (2022). Contribution Ratio Assessment of Process Parameters on Robotic Milling Performance. *Materials*, *15*(10). https://doi.org/10.3390/ma15103566

Piska, M., & Urbancova, K. (2022). On the Machining of Joint Implant UHMWPE Inserts. *MATEC Web of Conferences*, *368*, 01012. https://doi.org/10.1051/matecconf/202236801012

Sun, H., Ding, H., Deng, C., & Xiong, K. (2023). Efficient Prediction of Stability Boundaries in Milling Considering the Variation of Tool Features and Workpiece Materials. *Sensors (Basel, Switzerland)*, *23*(21). https://doi.org/10.3390/s23218954

Wan Jusoh, W. N. S. E., Yahaya, M. I., Zakaria, S., Mahamad Basri, M. H., Daud, M. R., & Ismail, N. I. (2025). Simulation-driven in robotic milling of soft material: Evaluating parallel and equidistant toolpath strategies using SprutCAM. *Academic Journal (EAJ) ESTEEM Academic Journal*, *22*, 64–80. https://doi.org/10.24191/esteem.v21iSeptember.6483.g4961

Wan Jusoh, W. N. S. E., Yahaya, M. I., Zakaria, S., Mahamd Basri, M. H., Daud, M. R., & Ismail, N. I. (2025). New approach to minimise surface roughness in Polytetrafluoroethylene (PTFE) through robotic spindle speed control. *ESTEEM Academic Journal*, *21*(March), 106–118. https://doi.org/10.24191/esteem.v21iMarch.4359.g3122

Wang, W., Guo, Q., Yang, Z., Jiang, Y., & Xu, J. (2023). A state-of-the-art review on robotic milling of complex parts with high efficiency and precision. *Robotics and Computer-Integrated Manufacturing*, *79*, 102436. https://doi.org/10.1016/j.rcim.2022.102436

Wen, J., Xie, F., Liu, X., & Yue, Y. (2023). Evolution and Development Trend Prospect of Metal Milling Equipment. In *Chinese Journal of Mechanical Engineering (English Edition)* (Vol. 36, Issue 1). Springer. https://doi.org/10.1186/s10033-023-00865-x

Wu, K., Li, J., Zhao, H., & Zhong, Y. (2022). Review of Industrial Robot Stiffness Identification and Modelling. In *Applied Sciences (Switzerland)* (Vol. 12, Issue 17). MDPI. https://doi.org/10.3390/app12178719

Yan, Z., Ren, X., Zhao, H., & Chen, S. (2024). Investigating the Impact of Robotic Milling Parameters on the Surface Roughness of Al-Alloy Fabricated by Wire Arc Additive Manufacturing. *Materials*, *17*(19). https://doi.org/10.3390/ma17194845